

Mechanical Properties of Epoxy Resin Based on Granite Stone Powder from the Sergipe Fold-and-Thrust Belt Composites

Jorge Antônio Vieira Gonçalves^{a*}, Diego Adalberto Teles Campos^b, Gislane de Jesus Oliveira^b,
Maria de Lourdes da Silva Rosa^c, Marcelo Andrade Macêdo^a

^aPrograma de Pós-graduação em Ciência e Engenharia de Materiais, Universidade Federal de Sergipe – UFS, São Cristóvão, SE, Brazil

^bDepartamento de Engenharia de Materiais, Universidade Federal de Sergipe – UFS, São Cristóvão, SE, Brazil

^cNúcleo de Geologia, Universidade Federal de Sergipe – UFS, Av. Marechal Rondon, s/n, Jardim Rosa Elze, CEP 49100-000, São Cristóvão, SE, Brazil

Received: July 10, 2013; Revised: April 26, 2014

This paper studies the mechanical properties including traction, flexion, compression, and hardness characteristics of a composite made from the combination of epoxy resin and granitic stone powder from the fold-and-thrust belt located in the municipality of Nossa Senhora da Glória, in the state of Sergipe, Brazil. Chemical and mineralogical analyses of the stone and analysis by SEM of the particle/matrix interface are performed. Two Granite types, named 53-A and 12-A, were incorporated with different mass percentages of 0%, 30% and 50%, in the polymeric matrix, DGEBA, formed by the Araldite polymer GY 279 and the curing agent Aradur 2963. The test results with 50% show a compression of 79 MPa with a maximum increase of 121% compared with the pure epoxy resin.

Keywords: epoxy resin, composite, mechanical properties, SEM

1. Introduction

Epoxy resins are highly reticulated thermosetting polymers which are easy to process, with high-performance, containing at least two epoxy groups per molecule¹⁻³. The epoxy ring is formed by two carbon atoms bonded to an oxygen atom, in which the angle of a C-O bond is 61°²⁴,^{14,51}, by means of a simple covalent bond⁶. Due to their high reactivity, epoxy rings may be used in several mechanical applications because of their good adhesive properties, rigidity, specific resistance, dimensional stability, chemical resistance and high fluidity prior to curing which allows for an easy processing⁷⁻¹². However, the curing process causes irreversible changes to the chemical and physical properties of the resin and hardener. Due to the formation of a highly crosslinked polymer, the resulting epoxy resins are usually fragile, brittle, and have low resistance to the propagation of cracks¹³⁻¹⁸.

A great deal of attention has been paid to the improvement of the mechanical properties of pure epoxy resin^{8,19-22}. This has included using many types of loads, such as glass particles, ceramics, silicates, and rubbers^{8,11,12,23-27} among others. The effects of the particle size, dispersion degree, filling interface, and filling volume have also been studied²³⁻²⁷. Combining suitable amounts of other materials allows the inherited properties of the components to contribute to the creation of new materials with adjusted and improved characteristics⁹.

A particulate composite may exhibit great variations in its mechanical resistance, and this may be influenced by a

large number of parameters. In particular, the mechanical resistance may be affected by the composite's size, chemical composition, shape, particle/matrix interface, and the dispersion of particles, in addition to the conditions of the tests and material manufacturing, the curing temperature, and the stoichiometric resin/hardener ratio^{8,13,28-31}.

This study proposes the use of feldspar-rich stone powder in order to produce a particulate composite, because it is favored by good adsorption with epoxy resin³². It aims to incorporate this stone powder in different mass percentages of 0%, 30%, and 50% as particles in the epoxy resin. The research will investigate the mechanical properties of the produced composite (with its tensile, flexural, compression, and hardness test), and study the particle/matrix interface and chemical composition of the powder.

2. Material and Methods

2.1. Materials

The used polymeric matrix is the Bisphenol A diglycidyl ether epoxy resin (DGEBA). It was cold cured. Before the curing process, it was a viscous liquid material formed of two parts. The first part is the polymer, Araldite GY 279, based on Bisphenol A, and the second one is the hardener, Aradur 2963, based on cycloaliphatic amine, both manufactured by Huntsman. Table 1 shows the characteristics of the resin.

For the development of the particulate composite two types of load were used: the granitic stone powders 53-A and 12-A, with specific surface area of 0.42 and 0.66m²/g,

*e-mail: javgdbg@gmail.com.br

respectively. These granitic stone powders came from the fold-and-thrust belt located in the municipality of Nossa Senhora da Glória in the state of Sergipe, Brazil, at Universal Transverse Mercator coordinates E=648131 and N=8907804 (53-A), and E=658636 and N=8879748 (12-A). The samples were made available in the form of rock fragments by the Department of Geology of the Federal University of Sergipe.

2.2. Method

2.2.1. Sample preparation

The polymer and the hardener were used in the proportions indicated by the manufacturer in order to provide the best mechanical performance. First, the powder was sieved using 106 μm brass mesh sieve. Next, the samples were placed in a Model 5 BrasDonto kiln for approximately 1 hour, at 100 °C, in order to remove water vapor. The powders were weighed and manually mixed with Araldite GY 279 BR in a beaker for 15 minutes using a glass stirring rod, prior to curing, in order to reduce the residual tension³³. Next, the Aradur 2963 was added to the mixture, and mixed together for another 15 minutes. Finally, the mixture was deposited into molds (for its tensile, flexural

and compression tests), which had previously been coated with solid vaseline.

The specimens were removed from the molds after 24 hours and, after 21 days (maximum time) of curing at room temperature, the mechanical tests were conducted. Figure 1 illustrates the procedure for manual molding used to manufacture the composites.

For a given composite application, the selection of the type of processing is always a challenge. These processes correspond to 50-60% of the total cost of the material produced. In addition, they significantly affect the microstructural distributions and, hence, the final properties of the composite, so this is a subject that demands significant attention from the industry and the scientific community^{1,34,35}.

The general manufacturing processes for epoxy particulate reinforced composites consist of mechanical shear mixing, ultrasound sonication, and other chemical and thermal methods, degassing under vacuum and the use of nanoparticles reinforcement, aiming at the reduction of viscosity and surface tension of the resin, thus increasing the overall level of dispersion of the particles in the epoxy matrix^{15,30,36-38}.

Table 1. The characteristics and proportions of the Polymeric system.

DETAILS	RESIN	CURE AGENT
Name	Araldite GY279	Aradur 2963
Base	Epoxy	Amine
Proportion	100	42
Density at 20 °C (g/cm3)	1.1	1.1
Viscosity at 25 °C (mPas)	500-700	30-70

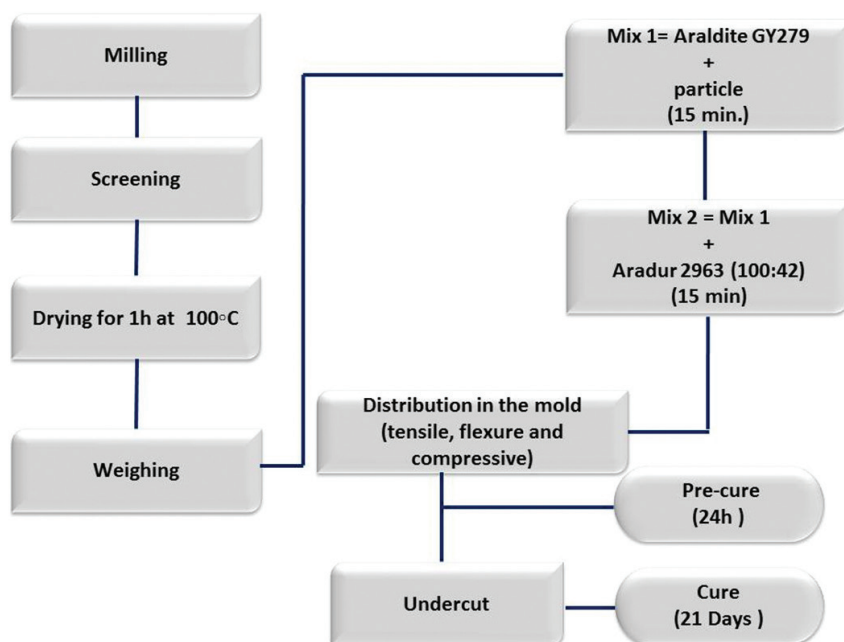


Figure 1. Flow diagram for the preparation of the particulate composites.

The control of the dispersion and homogeneity status in the distribution of particles in the matrix, the formation of agglomerates, the understanding of the effect of the interface between the matrix and the reinforcement are the main limitations in manufacturing processes of particulate polymeric composites^{39,40}.

When we add reinforcement to a polymer, almost all properties are affected, some positively, others negatively, in relation to a particular application⁴¹.

A simple mixing process was implemented through manual agitation, in order to reduce the residual stresses of the cured epoxy resin, the particles were first dispersed in the polymer and, subsequently, with the hardener⁴².

The manufacturing process used can be the cause of the reduction of some mechanical properties, a situation that was detected by other researchers who used simple mechanical stirrer, causing the lack of adequate dispersion of the particles given the low energy provided to generate the required shear stress³⁰; consequently, the ideal condition in which all the particles should be fully covered by the epoxy matrix may not have been fully satisfied.

On the other hand, the size and shape of the particles, the aspect ratio, the natural tendency of particles to agglomerate and the moisture absorption also play a major role in the mechanical performance^{30,39,40}.

Industrial scale processes can significantly improve the mechanical properties, due to its greater capacity of distributing the particles. Among the techniques for manipulating the particles, we can mention the flow through bins and pneumatic molds, which through the simultaneous disturbance and vibration can make smaller particles occupy the interstices between the larger particles so as to achieve a high packing density³⁴.

However, the hand mixing process was chosen because of its advantages, such as low investment, easy handling, molding in various sizes and thicknesses, possibility of use in various applications and reproducibility of the process. This last advantage can be demonstrated with the calculation of the coefficient of variation that estimates the accuracy of the results, in which a percentage lower than 20% was found, corresponding to a lower value than the one generally found, since the variability of the results is inherent to the manufacturing process⁶.

2.3. Mechanical test

All mechanical tests were conducted in the laboratory at the Materials Science and Engineering Department of the Federal University of Sergipe. For the traction and bending tests, an Instron 3367 universal testing machine was used, and for compression test, an Instron 3385H universal testing machine was used.

2.3.1. Tensile

In the tensile test, the load cell used was 30 kN, at a speed of 5 mm/min. Six dumbbell-shaped specimens were used with the dimensions of 105±2 mm long, 10±2 mm length, and 4±2 mm thick, in accordance with the ISO 527-2E standard⁴³. The tensile strengths were calculated by using Equation 1:

$$\sigma = F/A \quad (1)$$

Where:

σ = tensile strength, MPa;

F = maximum load, N;

A = average cross-sectional area, m².

2.3.2. Flexure

The mechanical three-point flexural test was adopted. A load cell of 5 kN was used, the distance between the two fixed points of support was 50 mm, and the speed was 2.00 mm/min. The six rectangular-shaped specimens were 80±2 mm long, 10±2 mm length and 4±2 mm thick, and they were used in accordance with the ISO 178:1993(E) standard⁴⁴. The loading was performed by a third mobile support positioned at an average distance of 40 mm from the rectangular specimen. The flexural strength determination was based on Equation 2:

$$\sigma = 3FL / (2bd^2) \quad (2)$$

where:

σ = flexural strength, MPa

F = rupture load, N

L = support span, m

b = width of specimen, m

d = thickness of specimen, m

2.3.3. Compression

In the compression test, the specimen was compressed resulting in a reduction of height. A load cell of 250 kN was used at a speed of 5 mm/min. The specimen had a cylindrical shape, and according to the ABNT NBR 5739/1980⁴⁵, 5 specimens with diameter of 50 mm and height of 100 mm were used. The compressive strength was calculated by using Equation 3:

$$f_c = 4F/\pi d^2 \quad (3)$$

Where:

f_c = compressive strength, MPa;

F = maximum load, N;

d = diameter of specimen, mm.

2.3.4. Hardness

The hardness of the polymeric composite is a critical parameter that influences the durability and lifespan of the material³³. A type-D Shore durometer was used to measure the samples, with a test range of 0 to 100 Shores, a tolerance of ±1%, and indenter dimensions of Ø 16 mm by 6.4 mm height, according to the ASTM D2240 standard⁴⁶. The hardness test consists of measuring the depth of the impression left in the composite, expressing its resistance to plastic deformation.

2.4. Microscopic analyses

For scanning electron microscopy (SEM), a Jeol JSM-6510LV scanning electron microscope was used to obtain images of the fractured surface. To this end, the samples were coated with a thin layer of gold deposited by a Denton Vacuum sputter.

2.5. XRF

Chemical analyses of the samples were made using X-ray fluorescence spectroscopy. The device used was a Bruker S8 TIGER. The tablets are 25 mm diameter, 4 mm thick, each of them containing 10g of powder.

2.6. DLS

Methods of the dynamic light scattering (DLS) measurements were performed by means of the Malvern Mastersize 2000 using the technique of laser diffraction to measure the size of particles. The measured autocorrelation functions were analyzed by Malvern DTS software.

3. Results and Discussion

3.1. Characterization

3.1.1. SEM and DLS

There is a natural tendency of the powder to form agglomerates due to its large superficial area (Figure 2a), preventing the full involvement of the matrix. This property might generate concentrations of tensions, and, consequently, a reduction in some mechanical properties.

The SEM micrographs area (Figure 2a and 3) shows that these particles are non-spherical, the influence of the

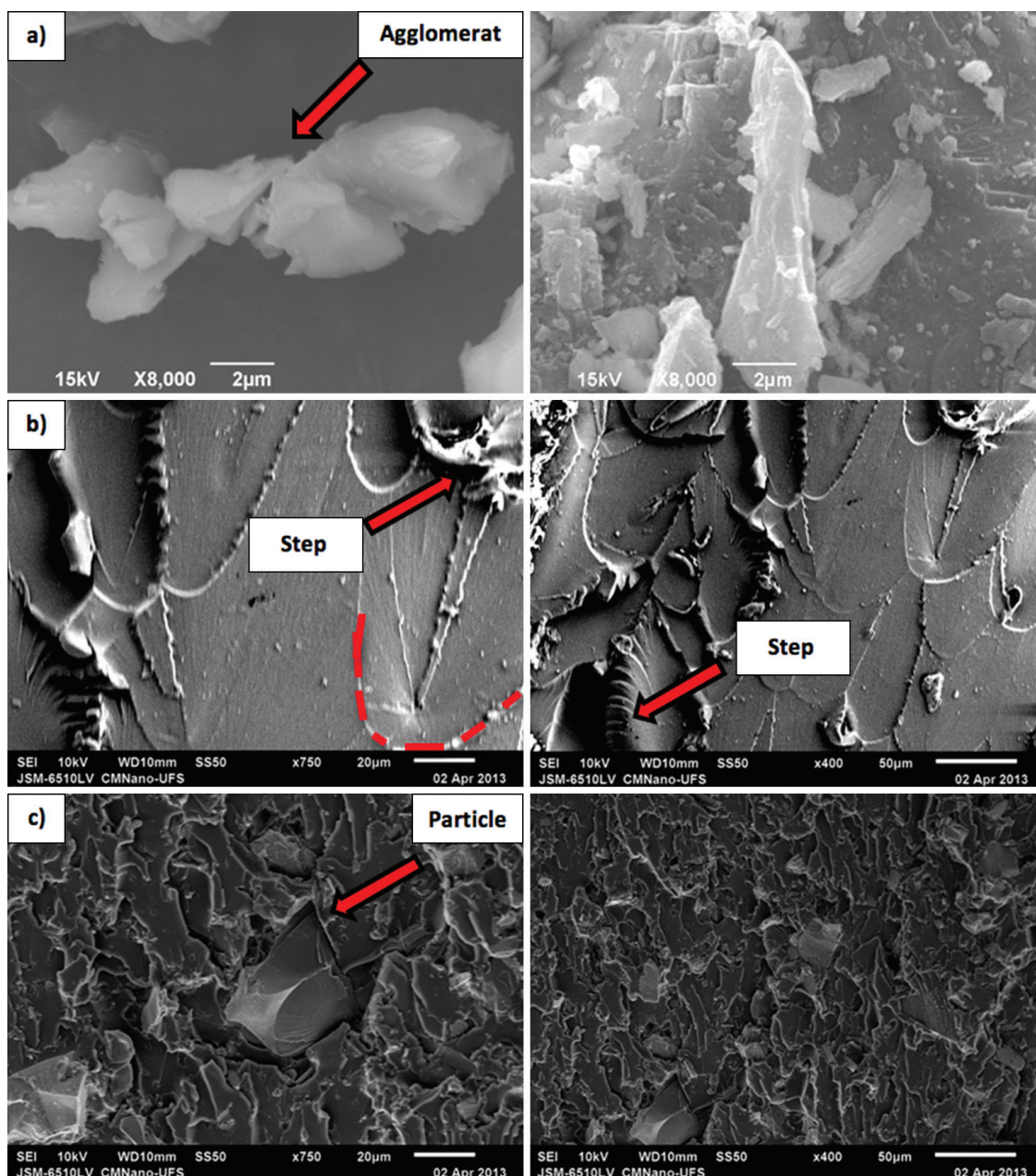


Figure 2. a) SEM images of the particles. b) The fractured surface of the pure epoxy resin. (c) The fractured surface with particles partially adhered to the matrix.

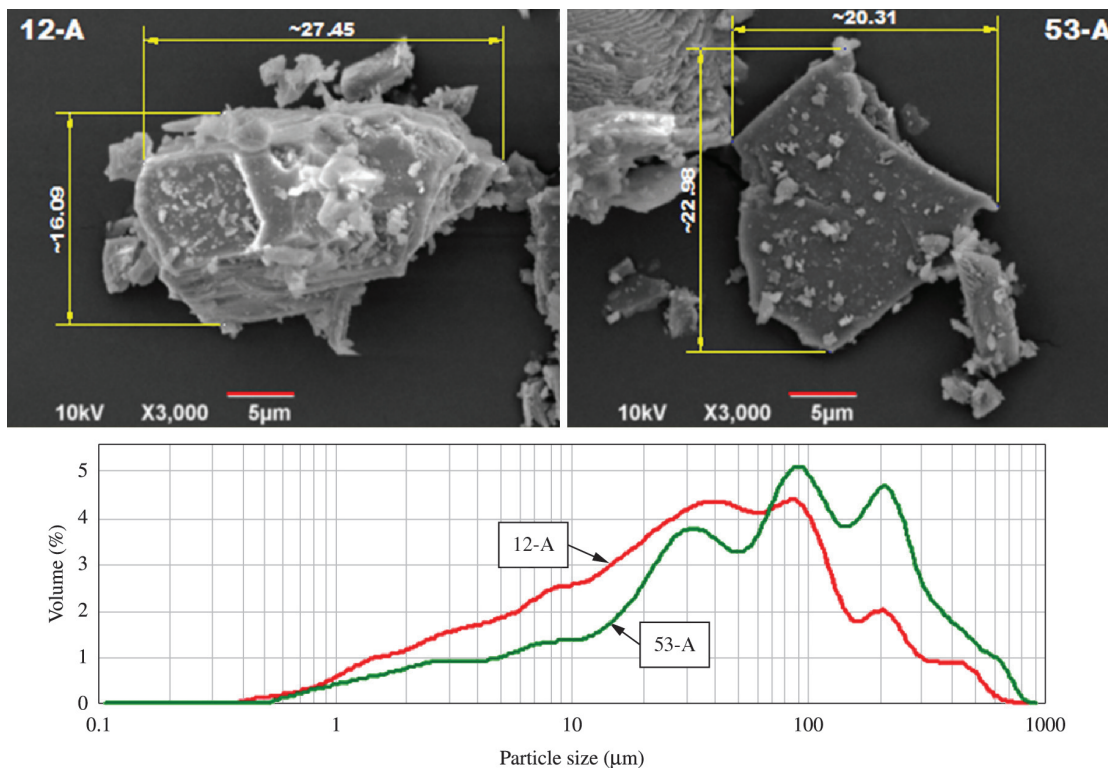


Figure 3. Particle size distribution after sieving.

shapes of the particles indicates that the larger and more irregular particles will cause discrepancies in the results of the analysis of grain sizes²⁹.

To find the packing density of the experimental techniques particles are subjected to segregation effects. Thus, the non-spherical fine particles are generally segregated to the bottom, which may be one of the causes of the difficulty in achieving better results of packing density³⁴.

The statistical results are reproduced in Table 2, from a Malvern Mastersizer, where the term $D(v,0.1)$ represents the particle diameter at which 10% of the distribution is below this value, the volume median diameter $D(v,0.5)$ is the diameter where 50% of the distribution is above and 50% is below, $D(v,0.9)$, 90% of the volume distribution is below this value.

Semi-elliptical marks⁴⁷ and steps (a shattering phenomenon that occurs in polymers with a low deformation capacity)⁶ were observed at the fracture surfaces of the pure epoxy resin (Figure 2b), causing flaws in the fragile, homogeneous material. In the images (Figure 2c), morphological changes in the composite microstructure are observed, indicating that the actual characteristics act as a sink to the applied load, thus improving the mechanical performance⁴⁸. The high rigidity of the particles (Figure 2c) modifies the natural propagation of cracks along the particle/matrix interface, preventing the cracks from penetrating places where particles are located⁴⁹.

3.1.2. Chemical and mineralogical analyses

The chemical composition of the rock samples used in this study is presented in Table 3. They comprise a high SiO_2

Table 2. Illustration of Malvern Statistical Results.

Mean diameters	12-A	53-A
$D(v,0.1)$ μm	3.36	6.13
$D(v,0.5)$ μm	32.43	69.31
$D(v,0.9)$ μm	164.29	281.42
Surface weighted Mean $D[3,2]$ μm	9.08	14.35
Volume weighted Mean $D[4,3]$ μm	64.70	115.02
Specific surface area m^2/g	0.66	0.42

(silicon dioxide) content and a high Al_2O_3 (aluminum oxide) content, with combined totals of 65.06% and 65.92% for the samples 53-A and 12-A, respectively. The high proportions of SiO_2 and Al_2O_3 obtained are typical of granitic stones⁵⁰. From a mineralogical point of view (Table 4), sample 53-A has the highest volumetric percentage of alkali feldspar ($(\text{K}, \text{Na})\text{AlSi}_3\text{O}_8$) reflecting a higher chemical content in Al_2O_3 , K_2O , and Na_2O . Likewise, the lower percentage of mafic minerals (biotite, hornblende, and augite) in these samples causes lower values for the oxides of Fe, Mg, and Ti.

3.2. Mechanical test

3.2.1. Tensile

Figure 4 and Table 5 show the fracture tension and average deformation values. There is a clear reduction of the strength in relation to the increasing amount of particles added to the system. The average modulus of elasticity increased 318% and 192% over pure epoxy resin after adding 50% loads of 53-A and 12-A, respectively.

Improvements in some properties, such as the longitudinal modulus of elasticity, are frequently associated with decreases in other properties, such as the limit of tensile strength, a fact that may be related to the loading in this test, facilitating the cracks due to instability⁴⁸. As can be observed in Figure 4, there is a reduction in the tensile strength limit when the amount of powder is increased; this behavior was

also observed by Fu et al.⁵¹. A low-particle/matrix¹³ adhesion and the high number of flaws occurring in the production phase (during the curing of the mixture)²⁸ are some of the main causes for this behavior. When the percentage of the load is increased, the degree of adhesion between the phases is reduced, demonstrating that there is a reduction in the transference of tension to dispersed-phase particles.

Table 3. Chemical analysis data from X-ray fluorescence spectroscopy.

53-A		12-A	
Formula	Weight (%)	Formula	Weight (%)
SiO ₂	51.94	SiO ₂	53.09
Al ₂ O ₃	13.11	Al ₂ O ₃	12.83
K ₂ O	4.63	Fe ₂ O ₃	5.03
Na ₂ O	3.35	K ₂ O	4.40
Fe ₂ O ₃	3.31	CaO	3.74
CaO	2.49	MgO	3.02
MgO	1.53	Na ₂ O	2.90
TiO ₂	0.49	TiO ₂	0.61
P ₂ O ₅	0.29	P ₂ O ₅	0.35
BaO	0.22	BaO	0.17

Table 4. Mineralogical composition of the samples.

53-A		12-A	
Minerals	(%)	Minerals	(%)
Alkali feldspar	47.1	Alkali feldspar	40.2
Quartz	26.6	Quartz	31.6
Plagioclase	9.4	Plagioclase	8.6
Hornblenda	8.3	Anfibólio	10
Biotita	7.6	Biotita	6.3
Augita	1	Piroxênio	3.3
Epídoto	< 0.1	Titanita	< 0.1
Titanita	< 0.1	Epidote	< 0.1
Apatite	< 0.1	Pyrite	< 0.1

3.2.2. Flexure

As observed in Figure 5 and Table 6, the average flexure and deformation values at the fracture decrease in relation to the increase in the amount of particles added to the system up to a percentage of 30% (similar to the tensile tests). After this percentage, the average flexure and deformation values increase again up to 50% of the load (similar to the compression tests). The average modulus of elasticity increases 230% and 188% over pure epoxy resin after adding 50% loads of 53-A and 12-A, respectively.

Sample 12-A has a smaller particle size and higher surface area, this particles tend to agglomerate more, resulting in a decreased interaction of matrix/filler composite which explains lower results regarding the sample 53-A⁵².

3.2.3. Compression

The best mechanical test results were the compression ones (in Figure 6 and Table 7); this fact might be related to the loading technique used in this test. The average strain break increases 121% and 65% over pure epoxy resin with the addition of 50% loads of 53-A and 12-A, respectively.

According to Yamini and Young¹⁹, there is an inconsistency among the results in the available literature due to the difficulty in controlling the propagation of cracks in epoxy resins. This is because they are predisposed to grow, sometimes in a continuous way (stable growth) and sometimes in pulses (unstable stick-slip growth).

When the particles are well dispersed, according to this percolation theory, there is a matrix zone around each particle affected by a stress concentration, if the distance between these particles is small enough, these zones join

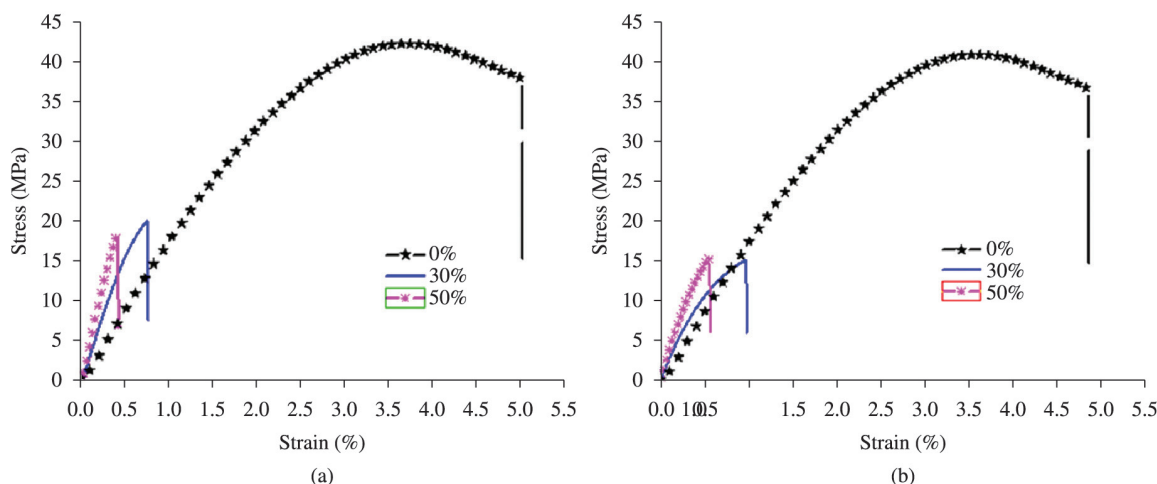
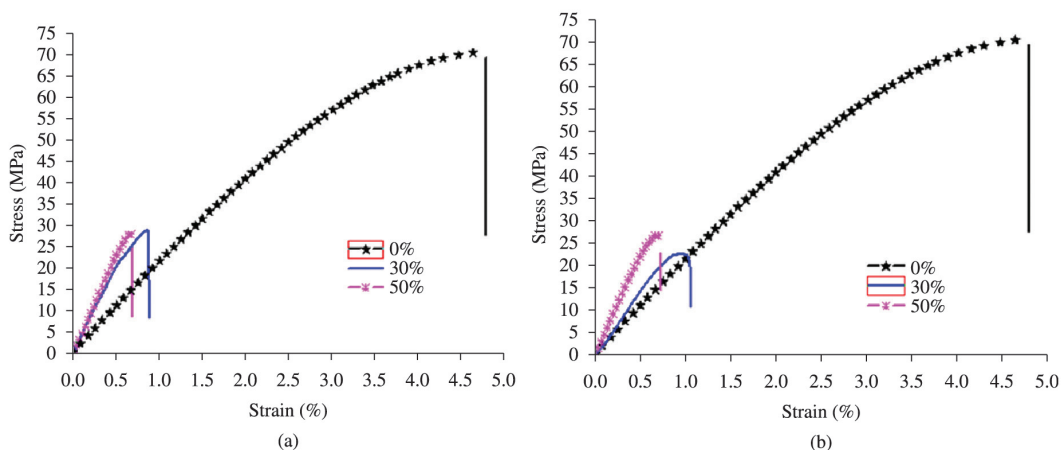


Figure 4. Tension-deformation curve illustrating the behavior under traction of polymeric systems for: a) epoxy resin and 53-A, and b) epoxy resin and 12-A.

Table 5. Results of the mechanical tensile tests.

System	Strain at Break (MPa)	Deformation at Fracture (%)	Modulus of Elasticity (GPa)
53-A			
0%	39.46 ± 3.75	3.80 ± 0.08	1.60 ± 0.29
30%	19.33 ± 0.93	0.69 ± 0.05	3.59 ± 0.13
50%	19.46 ± 1.09	0.43 ± 0.04	5.10 ± 0.21
12-A			
0%	39.46 ± 3.75	3.80 ± 0.08	1.60 ± 0.29
30%	14.92 ± 1.91	0.97 ± 0.10	1.98 ± 0.10
50%	14.58 ± 0.99	0.56 ± 0.05	3.08 ± 0.10

**Figure 5.** Tension-deformation curves illustrating the behavior under flexure of polymeric systems for: a) epoxy resin and 53-A, and b) epoxy resin and 12-A.**Table 6.** Results of the mechanical flexure tests.

System	Strain at Break (MPa)	Deformation at Fracture (%)	Modulus of Elasticity (GPa)
53-A			
0%	69.12 ± 2.75	4.92 ± 0.09	1.92 ± 0.04
30%	26.75 ± 2.47	0.97 ± 0.07	3.01 ± 0.29
50%	27.68 ± 3.28	0.73 ± 0.09	4.42 ± 0.34
12-A			
0%	69.12 ± 2.75	4.92 ± 0.09	1.92 ± 0.04
30%	21.82 ± 1.62	1.12 ± 0.31	2.38 ± 0.41
50%	22.31 ± 3.75	0.69 ± 0.10	3.61 ± 0.58

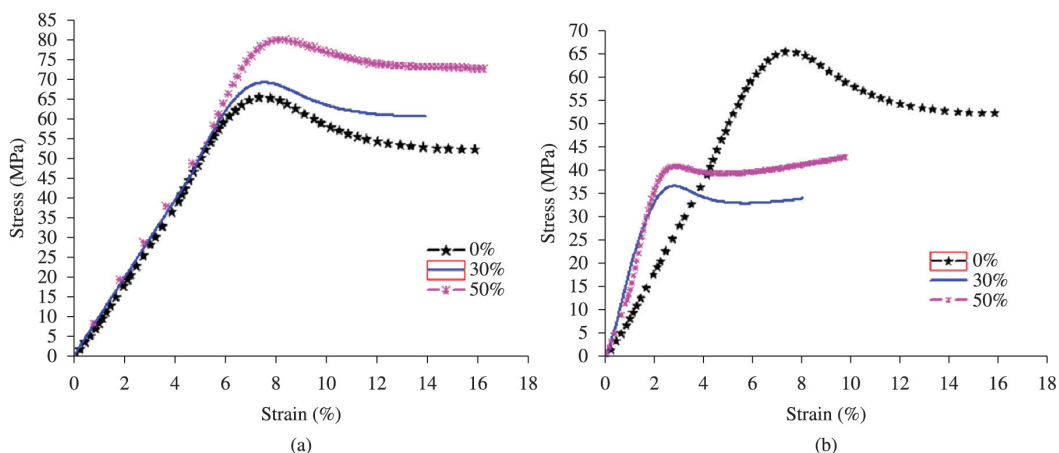
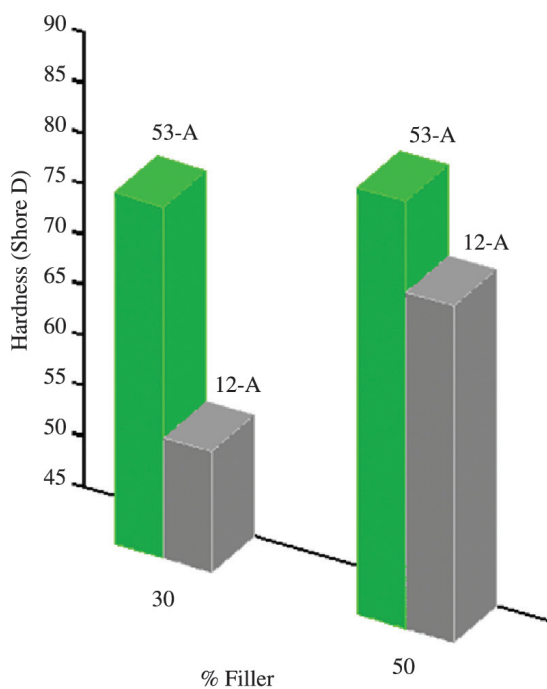
**Figure 6.** Tension-deformation curves illustrating the behavior under compression of polymeric systems for: a) epoxy resin and 53-A, and b) epoxy resin and 12-A.

Table 7. Results of the mechanical compression test.

System	Strain at Break (MPa)	Deformation at Fracture (%)	Modulus of Elasticity (GPa)
53-A			
0%	65.52 ± 0.29	16.32 ± 0.45	1.31 ± 0.03
30%	69.22 ± 1.09	14.67 ± 0.97	1.49 ± 0.02
50%	79.33 ± 0.98	15.69 ± 1.20	1.68 ± 0.06
12-A			
0%	65.52 ± 0.29	16.32 ± 0.45	1.31 ± 0.03
30%	37.36 ± 0.53	8.45 ± 0.51	1.18 ± 0.05
50%	42.96 ± 2.40	8.28 ± 0.85	1.42 ± 0.09

**Figure 7.** Variation of hardness with fillers.

together and form a percolation network, therefore the modulus of elasticity increases⁵².

3.2.4. Hardness

By examining the results of the hardness tests, it was found that, by increasing the percentage of the load in the pure epoxy resin up to 50%, the hardness of the composite increased³³ by 87.3 and 78.3 Shores (D-type) for the samples 53-A and 12-A, respectively. This behavior might

be attributed to the high rigidity of the dispersed-phase particles (Figure 7).

4. Conclusion

Following the analysis of the results, it was possible to get to the following conclusions:

- Improvements in some properties are frequently followed by a decrease in other properties.
- In the tensile test, the elastic modulus increased by an average of 318% and 192% over pure epoxy resin with the addition of 50% loads of 53-A and 12-A, respectively. With the lowering of the tensile strength, which might be related to the load of this test, causing the propagation of cracks, a similar situation occurs in the flexural test with 30% load.
- In the compression test, compressive strength average increases 121% and 65% over pure epoxy resin with the addition of 50% loads of 53-A and 12-A, respectively, in accordance with this percolation theory.
- The modulus of all the composites increased as granite powder content increases.
- The hardness increased 139% and 125% over pure epoxy resin with the addition of 50% loads of 53-A and 12-A, respectively. This behavior might be attributed to the high rigidity of the dispersed-phase particles
- Samples using the 53-A powder showed better performance in their mechanical properties. This behavior might be associated with the higher volumetric percentage of alkali feldspar [(K, Na) AlSi₃O₈].
- In future research, the modification of granite powder can lead to improved particle/matrix interaction promoting the improvement in the mechanical properties of the composite.

References

1. Neto FL and Pardini LC. *Compósitos Estruturais: Ciência e tecnologia*. São Paulo: Editora Edgard Blucher; 2006.
2. Lokensgard E. *Plásticos Industriais: Teoria e aplicações*. 5. ed. São Paulo: CENGAGE Learning; 2013.
3. Mano EB. *Polímeros como Materiais de Engenharia vol. 1*. São Paulo: Editora Edgard Blucher; 1991.
4. Grob A, Kollek H, Schormann A and Brockmann H. Spectroscopical contributions to the regioselectivity of nucleophilic curing reactions in epoxy resins. *International Journal of Adhesion and Adhesives*. 1988; 8(3):147-158. [http://dx.doi.org/10.1016/0143-7496\(88\)90093-0](http://dx.doi.org/10.1016/0143-7496(88)90093-0)
5. Almeida JRM, Monteiro SN. Efeito da variação da Razão Resina/Endurecedor sobre a Resistência ao Impacto de uma Resina Epóxi. *Polímeros*. 1996; 6(1):44-49.
6. Sobrinho LL. *Desenvolvimento de tubos compósitos para possíveis aplicações como risers*. [Tese]. Rio de Janeiro: Universidade Federal do Rio de Janeiro; 2009.
7. Segovia F, Salvador MD, Amigó V and Vicente A. Cure effects on post-impact tensile characteristics of 2D epoxy composites. *Journal of Materials Processing Technology*. 2003; 143-144:209-213. [http://dx.doi.org/10.1016/S0924-0136\(03\)00422-9](http://dx.doi.org/10.1016/S0924-0136(03)00422-9)
8. Xing XS and Li RKY. Wear behavior of epoxy matrix composites filled with uniform sized sub-micron spherical silica particles. *Wear*. 2004; 256(1-2):21-26. [http://dx.doi.org/10.1016/s0043-1648\(03\)00220-5](http://dx.doi.org/10.1016/s0043-1648(03)00220-5)
9. Deng S, Zhang J, Ye L and Wu J. Toughening epoxies with halloysite nanotubes. *Polymer*. 2008; 49(23):5119-5127. <http://dx.doi.org/10.1016/j.polymer.2008.09.027>
10. Kim BC, Park SW and Lee DG. Fracture toughness of the nano-particle reinforced epoxy composite. *Composite Structures*. 2008; 86(1-3):69-77. <http://dx.doi.org/10.1016/j.compstruct.2008.03.005>
11. Hsieh TH, Kinloch AJ, Masania K, Taylor AC and Sprenger S. The mechanisms and mechanics of the toughening of epoxy polymers modified with silica nanoparticles. *Polymer*. 2010; 51:26, 6284-6294. <http://dx.doi.org/10.1016/j.polymer.2010.10.048>
12. Monteiro SN, Menezes GW, Skury ALD, Lopes FPD, Rodriguez RJS and Bobrovitchii GS. Propriedades mecânicas e termomecânicas de compósitos com partículas de diamante dispersas em matriz epoxídica modificada na razão resina/endurecedor. *Matéria (Rio de Janeiro)*. 2006; 11:385-394.
13. Olmos D, Aznar AJ and González-Benito J. Kinetic study of the epoxy curing at the silica particles/epoxy interface using the fluorescence of pyrene label. *Polymer Testing*. 2005; 24(3):275-283. <http://dx.doi.org/10.1016/j.polymertesting.2004.11.008>
14. Dittanet P and Pearson RA. Effect of silica nanoparticle size on toughening mechanisms of filled epoxy. *Polymer*. 2012; 53(9):1890-1905. <http://dx.doi.org/10.1016/j.polymer.2012.02.052>
15. Wetzel B, Rosso P, Hauptert F and Friedrich K. Epoxy nanocomposites - fracture and toughening mechanisms. *Engineering Fracture Mechanics*. 2006; 73(16):2375-2398. <http://dx.doi.org/10.1016/j.engfracmech.2006.05.018>
16. Roşu D, Caşcaval C N, Mustaţă F and Ciobanu C. Cure kinetics of epoxy resins studied by non-isothermal DSC data. *Thermochimica Acta*. 2002; 383(1-2):119-127. [http://dx.doi.org/10.1016/S0040-6031\(01\)00672-4](http://dx.doi.org/10.1016/S0040-6031(01)00672-4)
17. Shadlou S, Alishahi E and Ayatollahi MR. Fracture behavior of epoxy nanocomposites reinforced with different carbon nano-reinforcements. *Composite Structures*. 2013; 95:577-581. <http://dx.doi.org/10.1016/j.compstruct.2012.08.002>
18. Jiang T, Kuila T, Kim NH, Ku B-C and Lee JH. Enhanced mechanical properties of silanized silica nanoparticle attached graphene oxide/epoxy composites. *Composites Science and Technology*. 2013; 79:115-125. <http://dx.doi.org/10.1016/j.compscitech.2013.02.018>
19. Yamini S and Young RJ. Stability of crack propagation in epoxy resins. *Polymer*. 1977; 18:10, 1075-1080. [http://dx.doi.org/10.1016/0032-3861\(77\)90016-7](http://dx.doi.org/10.1016/0032-3861(77)90016-7)
20. Pardini LC. *Comportamento dinâmico mecânico e fratura de materiais compostos epóxi/elastômero/fibra de carbono*. [Tese]. São Paulo: Instituto Tecnológico de Aeronáutica; 1990.
21. Danusso F and Tieghi G. Strength versus composition of rigid matrix particulate composites. *Polymer*. 1986; 27(9):1385-1390. [http://dx.doi.org/10.1016/0032-3861\(86\)90038-8](http://dx.doi.org/10.1016/0032-3861(86)90038-8)
22. Lapique F and Redford K. Curing effects on viscosity and mechanical properties of a commercial epoxy resin adhesive. *International Journal of Adhesion and Adhesives*. 2002; 22(4):337-346. [http://dx.doi.org/10.1016/s0143-7496\(02\)00013-1](http://dx.doi.org/10.1016/s0143-7496(02)00013-1)
23. Elaloui O, Ghorbel E, Mignot V and Ben Ouedzou M. Mechanical and physical properties of epoxy polymer concrete after exposure to temperatures up to 250°C. *Construction and Building Materials*. 2012; 27(1):415-424. <http://dx.doi.org/10.1016/j.conbuildmat.2011.07.027>
24. Jiao W, Liu Y and Qi G. Studies on mechanical properties of epoxy composites filled with the grafted particles PGMA/Al₂O₃. *Composites Science and Technology*. 2009; 69(3-4):391-395. <http://dx.doi.org/10.1016/j.compscitech.2008.11.003>
25. Panzera TH, Sabariz ALR, Strecker K, Borges PHR, Vasconcelos DCL and Wasconcelos WL. Mechanical properties of composite materials based on Portland cement and epoxy resin. *Cerâmica*. 2010; 56:77-82.
26. Li H, Zhang Z, Ma X, Hu M, Wang X and Fan P. Synthesis and characterization of epoxy resin modified with nano-SiO₂ and γ -glycidioxypropyltrimethoxy silane. *Surface and Coatings Technology*. 2007; 201(9-11):5269-5272. <http://dx.doi.org/10.1016/j.surfcoat.2006.07.143>
27. Al-Turaif HA. Effect of nano TiO₂ particle size on mechanical properties of cured epoxy resin. *Progress in Organic Coatings*. 2010; 69(3):241-246. <http://dx.doi.org/10.1016/j.porgcoat.2010.05.011>
28. Borsellino C, Calabrese L and Di Bella G. Effects of powder concentration and type of resin on the performance of marble composite structures. *Construction and Building Materials*. 2009; 23(5):1915-1921. <http://dx.doi.org/10.1016/j.conbuildmat.2008.09.005>
29. Xu R and Di Guida OA. Comparison of sizing small particles using different technologies. *Powder Technology*. 2003; 132(2-3):145-153. [http://dx.doi.org/10.1016/s0032-5910\(03\)00048-2](http://dx.doi.org/10.1016/s0032-5910(03)00048-2)
30. Dong Y, Chaudhary D, Ploumis C and Lau K-T. Correlation of mechanical performance and morphological structures of epoxy micro/nanoparticulate composites. *Composites Part A: Applied Science and Manufacturing*. 2011; 42(10):1483-1492. <http://dx.doi.org/10.1016/j.compositesa.2011.06.015>
31. Conradi M, Zorko M, Kocijan A and Verpoest I. Mechanical properties of epoxy composites reinforced with a low volume fraction of nanosilica fillers. *Materials Chemistry and Physics*. 2013; 137(3):910-915. <http://dx.doi.org/10.1016/j.matchemphys.2012.11.001>
32. Rachele KG, Correia JCG and Ribeiro RCC. Determinação das Condições para Otimização do Processo de Resinagem. In:

- Anais do XVII Jornada de Iniciação Científica – CETEM*; 2009; Rio de Janeiro. CETEM; 2009.
33. Ma S, Gibson I, Balaji G and Hu QJ. Development of epoxy matrix composites for rapid tooling applications. *Journal of Materials Processing Technology*. 2007; 192-193:75-82. <http://dx.doi.org/10.1016/j.jmatprotec.2007.04.086>
 34. Fiske TJ, Railkar SB and Kalyon DM. Effects of segregation on the packing of spherical and nonspherical particles. *Powder Technology*. 1994; 81(1):57-64. [http://dx.doi.org/10.1016/0032-5910\(94\)02862-1](http://dx.doi.org/10.1016/0032-5910(94)02862-1)
 35. Erol M and Kalyon DM. Assessment of the Degree of Mixedness of Filled Polymers. *International Polymer Processing*. 2005; 20(3):228-237. <http://dx.doi.org/10.3139/217.1882>
 36. Zhao S, Schadler LS, Duncan R, Hillborg H and Auletta T. Mechanisms leading to improved mechanical performance in nanoscale alumina filled epoxy. *Composites Science and Technology*. 2008; 68(14):2965-2975. <http://dx.doi.org/10.1016/j.compscitech.2008.01.009>
 37. Yasmin A, Luo JJ, Abot JL and Daniel IM. Mechanical and thermal behavior of clay/epoxy nanocomposites. *Composites Science and Technology*. 2006; 66(14):2415-2422. <http://dx.doi.org/10.1016/j.compscitech.2006.03.011>
 38. Yasmin A, Abot JL and Daniel IM. Processing of clay/epoxy nanocomposites by shear mixing. *Scripta Materialia*. 2003; 49(1):81-86. [http://dx.doi.org/10.1016/S1359-6462\(03\)00173-8](http://dx.doi.org/10.1016/S1359-6462(03)00173-8)
 39. Allahverdi A, Ehsani M, Janpour H and Ahmadi S. The effect of nanosilica on mechanical, thermal and morphological properties of epoxy coating. *Progress in Organic Coatings*. 2012; 75(4):543-548. <http://dx.doi.org/10.1016/j.porgcoat.2012.05.013>
 40. Pascault J-P and Williams RJJ. *Epoxy Polymers New Materials and Innovations*. Germany; 2010.
 41. Leblanc JL. *Filled Polymers Science and Industrial Applications*. United States of America, Taylor and Francis Group, LLC; 2010.
 42. Lai M, Friedrich K, Botsis J and Burkhart T. Evaluation of residual strains in epoxy with different nano/micro-fillers using embedded fiber Bragg grating sensor. *Composites Science and Technology*. 2010; 70(15):2168-2175. <http://dx.doi.org/10.1016/j.compscitech.2010.08.019>
 43. International Organization for Standardization – ISO. *ISO 527-2(E)*: Plastics - Determination of tensile properties - Part 2: Test conditions for moulding and extrusion plastics. ISO; 1993.
 44. International Organization for Standardization – ISO. *ISO 178(E)*: Plastics - Determination of flexural properties. ISO; 1993.
 45. Associação Brasileira de Normas Técnicas – ABNT. *ABNT NBR 5739*: Concreto – Ensaio de Compressão de corpos-de-prova cilíndricos. ABNT; 1980.
 46. American Society for Testing and Materials – ASTM. *ASTM D 2240*: Standard Test Method for Rubber Property – Durometer Hardness. West Conshohocken; 2005.
 47. Lin YC and Chen X. Investigation of the effect of hygrothermal conditions on epoxy system by fractography and computer simulation. *Materials Letters*. 2005; 59(29-30):3831-3836. <http://dx.doi.org/10.1016/j.matlet.2005.06.061>
 48. Li X, Zhan Z-J, Peng G-R and Wang W-K. New high-performance epoxy nanocomposites co-reinforced by two- and zero-dimensional nanoscale particles. *Materials Science and Engineering: A*. 2011; 530:680-684. <http://dx.doi.org/10.1016/j.msea.2011.09.111>
 49. Silva LJ, Panzera TH, Christoforo AL, Rubio JCC and Scarpa F. Micromechanical analysis of hybrid composites reinforced with unidirectional natural fibres, silica microparticles and maleic anhydride. *Materials Research*. 2012; 15:1003-1012.
 50. Moreira JMS, Freire MN and Holanda JNF. Utilização de resíduo de serragem de granito proveniente do estado do Espírito Santo em cerâmica vermelha. *Cerâmica*. 2003; 49:262-267.
 51. Fu S-Y, Feng X-Q, Lauke B and Mai Y-W. Effects of particle size, particle/matrix interface adhesion and particle loading on mechanical properties of particulate-polymer composites. *Composites Part B: Engineering*. 2008; 39(6):933-961. <http://dx.doi.org/10.1016/j.compositesb.2008.01.002>
 52. Ramakrishna HV, Priya SP and Rai SK. Flexural, compression, chemical resistance, and morphology studies on granite powder-filled epoxy and acrylonitrile butadiene styrene-toughened epoxy matrices. *Journal of Applied Polymer Science*. 2007; 104(1):171-177. <http://dx.doi.org/10.1002/app.25115>